Korean J. Chem. Eng., 39(2), 263-274 (2022)
DOI: 10.1007/s11814-021-0937-7

pISSN: 0256-1115
eISSN: 1975-7220

Temperature driven internal heat integration in an energy-efficient partial double annular column

Chaeyeong Seo, Heecheon Lee, Minyong Lee, and Jae W. Lee†

Department of Chemical & Biomolecular Engineering, Korea Advanced Institute of Science and Technology (KAIST), 291 Daehak-ro, Daejeon 34141, Korea

(*Received 15 March 2021 • Revised 4 August 2021 • Accepted 24 August 2021*)

Abstract−This study presents a strategy for the internal heat integration of reactive distillation (RD) columns for concurrently producing 2-ethylhexyl dodecanoate and methyl dodecanoate. Because of a significant temperature difference in the two reactions, the two RD column process with each single reaction occurring in the respective column has lower energy consumption than the direct sequence consisting of one RD column followed by a non-RD column. Thus, internal heat integration in a partial double annular configuration is introduced on the basis of the two RD column process. In the new annular RD configuration, heat is transferred from the outer column shell having a high-temperature exothermic reaction to the inner shell with a low-temperature endothermic reaction. By using the concept of pinch temperature, we determine the heat transfer stages to secure sufficient temperature driving force. For the same product purity and reaction extent, the internal heat integrated distillation column (HIDiC) shows lower internal flowrate and energy consumption than the other sequences of the direct sequence and the reactive dividing wall column (RDWC). The total utility consumption of the HIDiC with a partial double annular structure was reduced by 15.4% and 14.4% compared to the direct sequence and the RDWC, respectively.

Keywords: Internal Heat Integration, Partial Double Annular Column, Heat Integrated Distillation Column, Reactive Distillation, Reactive Dividing Wall Column

INTRODUCTION

As global warming is accelerating, research on CO_2 utilization and efficient energy use is being actively conducted [1,2]. Distillation is an essential separation process to meet product specifications in chemical process design [3,4]. However, it requires a large amount of energy and consumes almost half of the entire energy in chemical industries [5]. Therefore, the energy savings in the distillation process is essential for sustainable operations. With regard to distillation, considerable efforts have been exerted related to reactive distillation (RD) since it offers several advantages by allowing both reaction and distillation in one column [6,7]. Intensifying two separate unit operations into a single shell can save capital and operating costs. The complete reaction conversion and high product selectivity are concurrently achievable by overcoming the limitation of reaction equilibrium through the continuous separation of products. The RD process can also circumvent the separation limitations such as the azeotropic points and distillation boundaries [8,9]. In terms of feasibility, the key challenge for circumventing each limitation is to understand the interaction between reaction and separation [10,11], and many graphical methods based on the concept of fixed points or transformed coordinates for designing RD have been proposed [12-14].

The dividing wall column (DWC) has several sections for separating multi-component mixtures by installing a wall inside the distillation column [15,16]. The DWC can save energy by reducing the number of condensers or reboilers, which allows the DWC to serve as a baseline for accompanying single or multiple reactions with less energy consumption [17,18]. By integrating the reaction to DWC, it can have both advantages of RD and DWC [19,20]. Thermal integration of conventional RD columns into a reactive dividing wall column (RDWC) can dramatically reduce energy consumption [21,22]. The RDWC for binary and ternary simultaneous production of n-butyl, n-amyl ester, and n-hexyl ester showed significant energy saving compared to the conventional RD [23,24].

Many approaches have been proposed to improve the energy efficiency of distillation processes such as external and internal heat integration [7,25]. As an example of external heat integration, a vapor recompression heat pump (VRHP) has shown significant energy savings [22]. In the case of diethyl carbonate production, the energy consumption of a RDWC integrated with a VRHP was reduced by 32.1% compared to a bare RDWC [26]. As well as external heat integration, internal heat integration is also being actively developed [27]. A heat integrated distillation column (HIDiC) can induce energy savings by exchanging heat between the internal parts of distillation columns [28]. In an HIDiC consisting of a stripper and a highly pressurized rectifier, the heat can be transferred from the high-temperature rectifier to the relatively low-temperature stripper due to the temperature gradient caused by a compressor. In a multiple column system, if there is a sufficient temperature difference between the columns caused by the operating pressure or even the reaction temperature, the HIDiC can be designed by integrating the high-temperature column and low-temperature column. If all or a part of the high-temperature section is in contact with the

†To whom correspondence should be addressed.
E-mail: jaewlee@kaist.ac.kr

low-temperature section by using heat panels, heat transfer between these two sections can occur. Energy savings of the HIDiC can thus be achieved.

The HIDiC with a double annular structure was first proposed by Glenchur and Govind in 1987 [29]. In the double annular model, the inner column and the outer annular column are in direct contact without using extra heat exchangers or heat panels for internal heat integration. Many processes with sufficient temperature difference have been studied for integration with this proposed structure [30,31]. A double annular structure for pressure swing azeotropic distillation was recently studied for internal heat integration through the column shells where the hot region provides heat to the cold region without any external equipment [32]. However, introducing internal heat integration into RD columns still remains a task due to the complication of combining reaction, separation, and heat transfer. This study introduces a partial double annular column for internal heat integration between two respective RD columns by using the operating temperature gradient. By transferring heat from the exothermic reaction in the high-temperature (HT) column to the endothermic reaction in the low-temperature (LT) column, heat utilization is more efficient and both reactions can have favorable reaction equilibrium. However, the column with an exothermic reaction must have a higher temperature profile than the other for heat transfer. In this study, a single HIDiC having a partial double annular structure with internal heat integration of two individual RD columns was proposed, as two reactions were carried out in each section. Adding the other heat integrated RD sequences, all processes were evaluated in terms of total utility consumption (TUC) and total annual cost (TAC).

REACTION AND FEASIBILITY STUDY

This study investigated two esterifications of exothermic and endothermic reactions to understand how they are integrated to enhance heat transfer. These two reactions have a large difference in reaction temperature and this may enable a sufficient temperature gradient to induce heat transfer. The two reaction systems consist of one common acid and two different alcohols (methanol (MEOH) and 2-ethylhexanol (2-EHOH)) with a large difference in boiling point. The exothermic reaction is the conversion of dodecanoic acid (DEAC) and 2-EHOH to 2-ethylhexyl dodecanoate (2-EHDEC) and water. The endothermic esterification of DEAC with MEOH yields methyl dodecanoate (MEDEC) and water. The reaction enthalpies were calculated based on the combustion enthalpies (refer to Supplementary Information).

$$C_{11}H_{23}COOH\ (DEAC)+C_8H_{17}OH\ (2\text{-}EHOH) \leftrightarrow C_{11}H_{23}\text{-}COO\text{-}C_8H_{17}\ (2\text{-}EHDEC)+H_2O \quad \Delta H=-11.0\ kJ/mol \quad (1)$$

$$C_{11}H_{23}COOH\ (DEAC)+CH_3OH\ (MEOH) \leftrightarrow C_{11}H_{23}\text{-}COO\text{-}CH_3\ (MEDEC)+H_2O \quad \Delta H=78.6\ kJ/mol \quad (2)$$

1. Thermodynamic and Kinetic Properties

We simulated two reactions in distillation columns by using Aspen Plus™ V11. The binary parameters of the UNIQUAC model to describe the phase equilibrium and kinetic parameters of the esterification were from the literature [33-35]. The UNIFAC estimation model was adopted to estimate the binary parameter unavailable in the UNIQUAC model. All binary interaction parameters for UNIQUAC model are listed in Table 1.

The kinetic data of two reactions based on activity are taken from prior studies [34,35]. Reactions (1) and (2) are based on the use of heterogeneous catalysts of sulphated zirconia (SZ) and Amberlyst 15, respectively. SZ has a higher maximum operating temperature (700 °C) than that of Amberlyst 15 (120 °C) [36]. The reaction rate equations of reactions (1) and (2) are shown below [34,35].

Table 1. UNIQUAC-binary parameters for the six components esterification system

Component *i*	Component *j*	A_{ij}	A_{ji}	B_{ij}	B_{ji}	C_{ij}	C_{ji}
[a]2-EHOH	DEAC	0	0	49.44	−52.77	0	0
[a]2-EHOH	WATER	11.517	−10	−785.57	−2.807	−1.718	1.5911
[a]2-EHOH	2-EHDEC	0	0	90.824	−183.25	0	0
[a]DEAC	WATER	−0.29924	−0.38437	−195.44	−107.62	0	0
[a]DEAC	2-EHDEC	0	0	97.72	−140.7	0	0
[a]WATER	2-EHDEC	−0.04839	−0.44196	−203.49	−738.1	0	0
[a]MEOH	DEAC	0	0	48.3493	−309.554	0	0
[a]MEOH	WATER	−1.0662	0.6437	432.879	−322.131	0	0
[a]MEOH	MEDEC	0	0	31.789	−539.979	0	0
[a]DEAC	WATER	−0.29924	−0.38437	−195.44	−107.62	0	0
[a]DEAC	MEDEC	0	0	238.847	−369.561	0	0
[a]WATER	MDEDC	0	0	−216.733	−658.816	0	0
[b]2-EHOH	MEOH	0	0	−225.063	31.7321	0	0
[b]2-EHOH	MEDEC	0	0	75.1972	−147.137	0	0
[b]2-EHDEC	MEOH	0	0	−580.607	18.528	0	0
[b]2-EHDEC	MEDEC	0	0	44.9103	−50.1052	0	0

[a]Literature data

[b]UNIFAC estimation for UNIQUAC binary parameter

Table 2. Singular points of esterification system in mass basis (at 1 atm); (a) Singular points for the four components of reaction (1); (b) Singular points for the four components of reaction (2); (c) Singular points for the six components of reactions (1) and (2)

(a)

Temp (°C)	Classification	Type*	DEAC	2-EHOH	2-EHDEC	WATER
99.134	Unstable node	AZ	0	0.190	0	0.810
100.017	Saddle	AZ	0	0	0.001	0.999
100.018	Saddle	Pure	0	0	0	1
184.453	Saddle	Pure	0	1	0	0
298.586	Saddle	Pure	1	0	0	0
334.497	Stable node	Pure	0	0	1	0

(b)

Temp (°C)	Classification	Type*	DEAC	MEOH	MEDEC	WATER
64.535	Unstable node	Pure	0	1	0	0
99.962	Saddle	AZ	0	0	0.023	0.977
100.018	Saddle	Pure	0	0	0	1
266.537	Saddle	AZ	0.031	0	0.969	0
266.624	Stable node	Pure	0	0	1	0
298.586	Stable node	Pure	1	0	0	0

(c)

Temp (°C)	Classification	Type*	DEAC	2-EHOH	2-EHDEC	MEOH	MEDEC	WATER
64.535	Unstable node	Pure	0	0	0	1	0	0
99.134	Saddle	AZ	0	0.190	0	0	0	0.810
99.962	Saddle	AZ	0	0	0	0	0.023	0.977
100.017	Saddle	AZ	0	0	0.001	0	0	0.999
100.018	Saddle	Pure	0	0	0	0	0	1
184.453	Saddle	Pure	0	1	0	0	0	0
266.537	Saddle	AZ	0.031	0	0	0	0.969	0
266.624	Saddle	Pure	0	0	0	0	1	0
298.586	Saddle	Pure	1	0	0	0	0	0
334.497	Stable node	Pure	0	0	1	0	0	0

*Pure: pure component and AZ: azeotrope

$$r_{(1)} = \left(k_U^* \frac{a_{DEAC}}{V_M} + k_C^* C_{cat}\right)\left(a_{DEAC}a_{2\text{-}EHOH} - \frac{a_{2\text{-}EHDEC}a_{WATER}}{K_a}\right)\frac{1}{V_M^2} \quad (3)$$

$$k_U^* = 163400e^{-65500/RT}$$

$$k_C^* = 3277e^{-55500/RT}$$

$$r_{(2)} = k_1 a_{DEAC}a_{EHOH} - k_{-1}a_{MEDEC}a_{WATER} \quad (4)$$

$$k_1 = 911640e^{-68710/RT}$$

$$k_{-1} = 14998e^{-64660/RT}$$

The liquid holdup was iteratively obtained with the constraint of reaction conversion, hydraulic column sizing, and minimum energy consumption. All stages of RD column were designed to be within the feasible operating range. Since both reactions had sufficient conversion at 0.05 m^3 of liquid holdup with feasible operation and minimum energy consumption, the liquid holdup was unified to 0.05 m^3 in two RD columns. The bulk density of SZ and Amberlyst 15 is 2,610 kg/m^3 and 1,050 kg/m^3, respectively [37,38]. The activity of component i (a_i) is the product of the activity coefficient (γ_i) and mole fraction (x_i).

2. Feasibility Study and Visualization for Distillation Processes

The singular points and dynamic properties of single components and azeotropes at 1 atm are summarized in Table 2. In Table 2(a), there are unstable and stable nodes for the four components system of reaction (1). The reacting mixture in reaction (2) has an unstable node and two stable nodes in Table 2(b). Since one distillation region should have a pair of an unstable node and a stable node [39], these two systems have one and two distillation regions, respectively. Fig. 1 shows that the compositional trajectory of each RD column reaches the pure product at both ends. The composition space of the 2-EHDEC production system has only one distillation region in Fig. 1(a) and it thus clearly separates two products at the top and bottom of one RD column.

However, it is difficult to separate the products from the reacting mixture in reaction (2) using a single RD column due to the distillation boundary in the quaternary composition, as shown in Fig. 1(b). To separate two products located in different distillation regions, the column profile should cross the distillation boundary. At the top of the RD column, the composition trajectory in the rectifying section is drawn to the zeotropic binary edge of the DEAC

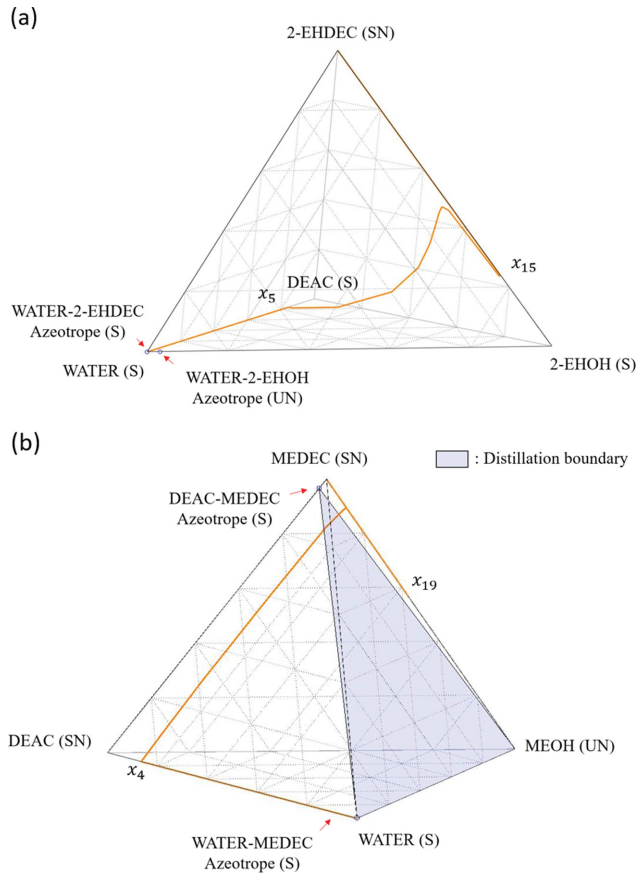

Fig. 1. Composition trajectories of quaternary system (a) in HT column with reaction (1) (b) in LT column with reaction (2).

and water by completely consuming MEOH in the stripping section. At the bottom of the RD column, the composition trajectory in the stripping section approaches the binary edge of the MEOH and MEDEC located in the other distillation region by consuming all DEAC. Thus, the single RD column can separate pure water and MEDEC at the top and bottom, respectively. For the case where the two reactions occur simultaneously in one RD column in Table 2(c), there is only one distillation region with a pair of an unstable node and a stable node, as in reaction (1).

ALTERNATIVE DESIGNS OF REACTIVE DISTILLATION COLUMNS

First, we designed two single RD columns where both endothermic and exothermic reactions occurred separately in the respective column: this is called a design sequence of the two RD columns process (Fig. 2(a)). This two-RD column process is compared to a direct sequence where the two esterification reactions proceed simultaneously in one RD column and the subsequent non-RD column separates the pure ester products (Fig. 2(b)). In the direct sequence, heat from the exothermic reaction may directly move to the endothermic reaction in the reactive stages. For a more energy efficient process, we further designed a new heat integrated configuration to drive more energy savings.

Before the simulation, we fixed feed streams to the same composition for all processes. For both reactions, the acid and alcohol were fed with a flow rate of 50 kmol/h. The flow rate was set to the default setting for all processes to minimize the number of variables and provide overall unity. In addition, the number of total stages (N_{Total}) was fixed at 25 and reaction stages (N_{RX}) of each column range from the 2nd to 24th stages initially. Detailed information for determining the stage number is described in Supplementary Information. Since MEOH and 2-EHOH are more volatile than DEAC, DEAC is fed to the upper feed stage than the other alcohols. The operating conditions of all processes are listed in Table 3. As shown in Table 3, the condenser pressure is 1 atm and the stage pressure drop is 0.0069 atm for all distillation columns. After design-

Table 3. Operating conditions and simulation results

Case	Single RD		Direct sequence	HIDiC	RDWC
	2-EHDEC	MEDEC			
Condenser pressure (atm)	1	1	1	1	1
Stage pressure drop (atm)	0.0069	0.0069	0.0069	0.0069	0.0069
[a]Bottoms rate of 1st column (kmol/h)	-	50	100	50	100
[a]Distillate rate of 1st column (kmol/h)	-	50	100	50	50
[a]Diameter of 1st column (m)	-	0.955	1.448	0.630	2.587
[a]Reflux ratio of 1st column	-	0.30	0.011	0.17	0.0055
[a]Boilup ratio of 1st column	-	1.18	0.83	0.44	5.97
[a]Liquid holdup of 1st column (m^3)	-	0.05	0.05	0.05	0.05
[b]Bottoms rate of 2nd column (kmol/h)	50	-	50	50	-
[b]Distillate rate of 2nd column (kmol/h)	50	-	50	50	50
[b]Diameter of 2nd column (m)	1.924	-	1.199	1.934	1.129
[b]Reflux ratio of 2nd column	0.49	-	0.88	0.00039	0.80
[b]Boilup ratio of 2nd column	4.14	-	1.88	3.85	3.09
[b]Liquid holdup of 2nd column (m^3)	0.05	-	-	0.05	-

[a]MEDEC producing column in single RD and HIDiC, RD column in direct sequence and RDWC
[b]2-EHDEC producing column in single RD and HIDiC, non-RD column in direct sequence and RDWC

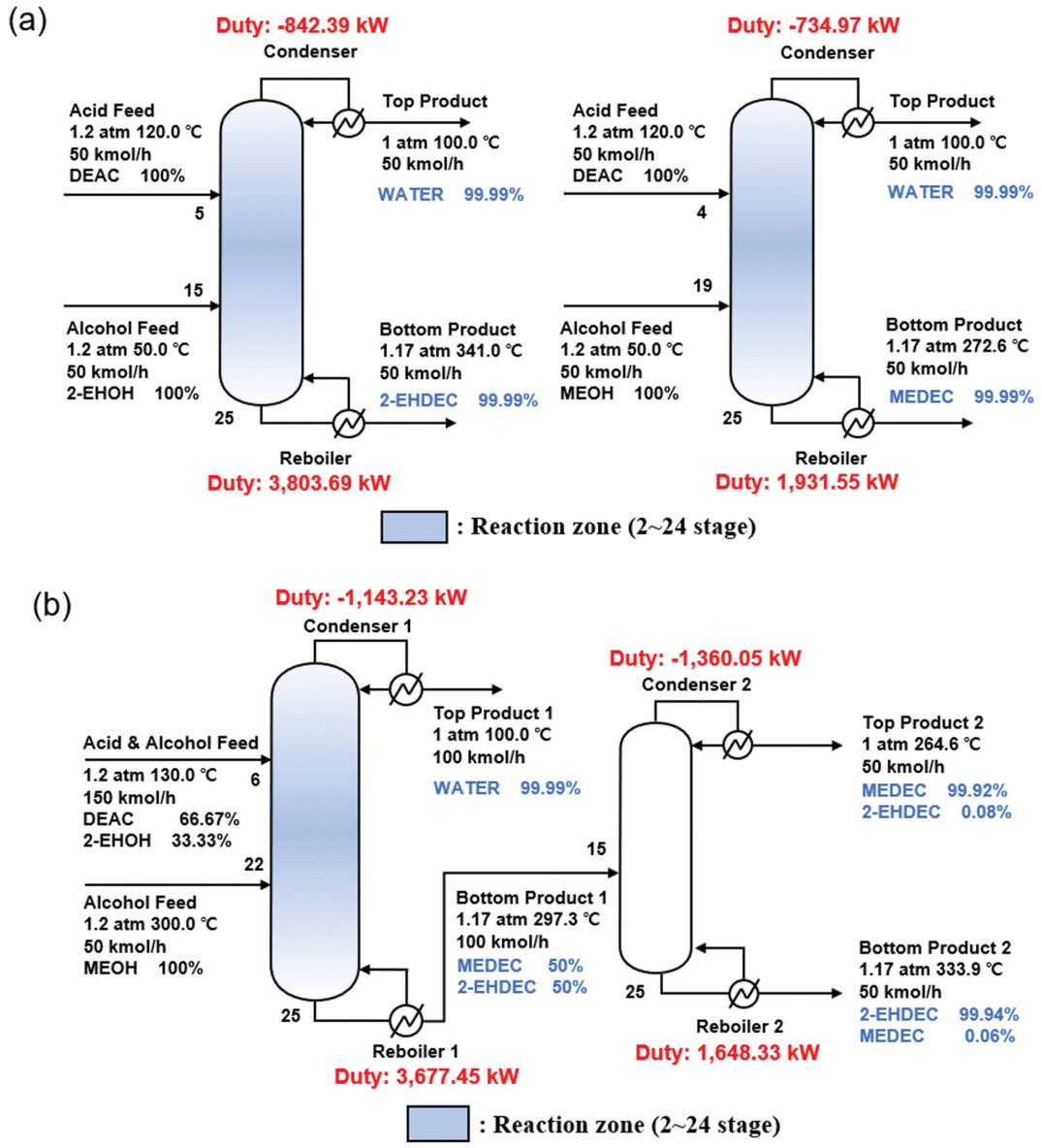

Fig. 2. Flowsheet of (a) two RD columns process and (b) conventional direct sequence.

ing all processes, we compared the reaction extent (ξ) to obtain the reaction conversion in each process. We also calculated TUC and TAC to compare the competitiveness of each process.

1. Two Reactions in Each Single RD Column and Simultaneously in One RD Column

Each single RD column producing a respective product of MEDEC and 2-EHDEC was designed according to the optimization procedure shown in Fig. 3. The optimal feed stages (NF_{ACID} and NF_{OH}) and reflux ratio of each column were determined so as to minimize TUC and TAC while producing ester products with a purity of 99.9 mol% or more. In the RD column for 2-EHDEC production, the feed stages of DEAC and 2-EHOH were the 5th and 15th stages, while DEAC and MEOH were injected to the 4th and 19th stages of the RD column for MEDEC production. The reflux ratios of the two respective RD columns were determined to be 0.30 for the 2-EHDEC case and 0.49 for the MEDEC case. To avoid excess use of catalyst, we minimized the number of reactive stages by figuring out the region where the reaction actually takes place within the RD column. For the same product purities, the optimized reactive stages were 10th to 24th stages for the HT column and 4th to 24th stages for the LT column. The simulation results of the two RD column process are shown in Fig. 2(a). All reactants were completely consumed due to the high reaction extent over 49.99 kmol/h in Table 4. The two single RD columns produced ester products with a purity of 99.99 mol% as a bottom product and pure water as a distillate product. As shown in Table 5, the RD column for 2-EHDEC production required a high reboiler duty of 3,803.69 kW, which is almost twice that of the MEDEC production case. Due to the differences in the reaction temperature and boiling points of 2-EHDEC (334.497 °C) and MEDEC (266.624 °C), the RD column for 2-EHDEC production has a higher temperature profile than the MEDEC production case (Fig. 4).

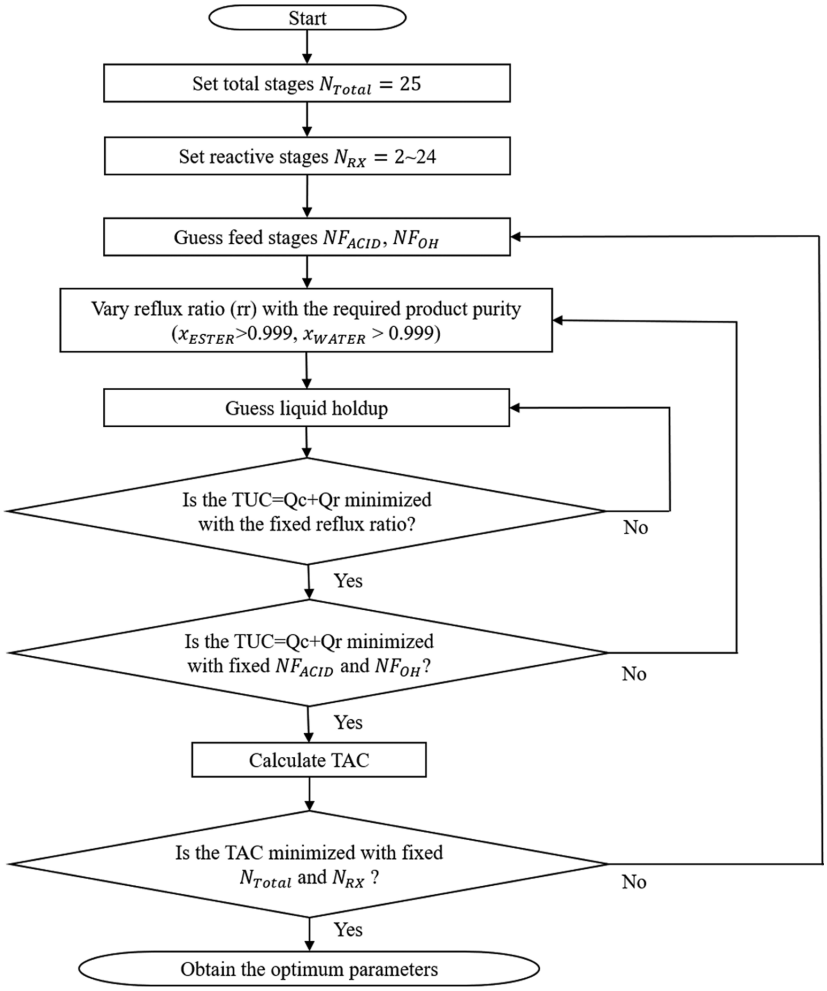

Fig. 3. Iterative optimization procedure of single RD column.

Table 4. Molar purities of products and reaction extents (ξ) of all processes

	Single RD	Direct sequence	HIDiC	RDWC
WATER	0.9999	0.9999	0.9999	0.9999
MEDEC	0.9999	0.9992	0.9999	0.9950
2-EHDEC	0.9999	0.9994	0.9999	0.9950
Reaction extent (ξ1), kmol/h	49.994	50	49.994	50
Reaction extent (ξ2), kmol/h	49.993	49.991	49.994	49.991

Table 5. Total utility consumption (TUC) of all processes

Utility (kW)		Single RD	Direct sequence	HIDiC	RDWC
[a]1st column	Condenser	−734.97	−1,143.23	−661.47	−1,136.97
	Reboiler	1,931.55	3,677.45	788.90	5,287.44
	TUC	2,666.52	4,820.68	1,450.37	6,424.41
[b]2nd column	Condenser	−842.39	−1,360.05	−579.30	−1,316.80
	Reboiler	3,803.69	1,648.33	4,595.97	-
	TUC	4,646.08	3,008.38	5,175.27	1,316.80
Total TUC		7,312.60	7,829.06	6,625.64	7,741.21

[a]MEDEC producing column in single RD and HIDiC, RD column in direct sequence and RDWC
[b]2-EHDEC producing column in single RD and HIDiC, non-RD column in direct sequence and RDWC

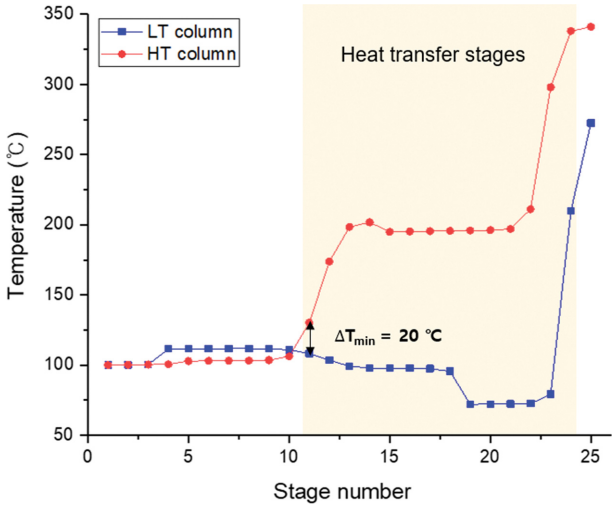

Fig. 4. Temperature profiles of two single RD columns for 2-EHDEC and MEDEC production.

These two separate processes with a common distillate byproduct of water can be integrated into a direct sequence where two esterification reactions occur simultaneously in one RD column unit [17,40]. The direct sequence in Fig. 2(b) consists of an RD column for the concurrent reaction and a non-RD column for separating the two ester products. Since the two catalysts (Amberlyst 15 and SZ) have different activation temperatures, they are not to be used simultaneously in one reactor. However, in this study, two catalysts are contained in one RD column of the direct sequence. In this RD column, it is assumed that Amberlyst 15 is thermally stable as the operating temperature of all stages is under 120 °C except for the two bottom stages. By separating water concurrently as a light common product and consuming reactants that form an azeotrope with other components, we can consider the non-RD column for separating the zeotropic mixture of two ester products. Each column was designed by the optimization procedure corresponding with that for the two RD column process. The reflux ratio of the RD column was 0.011 and that of the non-RD column was 0.879. The feed stages of DEAC and 2-EHOH were both the 6th stage and that of MEOH was the 22nd stage.

As shown in Table 4, the reaction extent of both reactions was sufficiently high (over 49.99 kmol/h) for both the two RD column process and the direct sequence. The ester product purities in the direct sequence (99.92 mol% and 99.94 mol%) were slightly lower than that of the two RD column process (99.99 mol%). As shown in Table 5, the sum of reboiler duties for the two RD column process was 5,735.24 kW, which was higher than that (5,325.78 kW) for the direct sequence. On the other hand, the sum of condenser duties for the direct sequence was 2,504.28 kW, which is 1.59 times higher than that (1,577.36 kW) of the two RD column process. In the direct sequence, two condensers handled a total flowrate of 150 kmol/h (100 kmol/h of common water on the RD column and 50 kmol/h of MEDEC on the non-RD column), whereas a total of 100 kmol/h of water (50 kmol/h on the single RD columns) was separated in the two RD columns process. For the same molar flowrate, MEDEC with a standard liquefaction enthalpy ($\Delta_{liq}H^o$) of −76.9 kJ/mol requires more energy consumption than water ($\Delta_{liq}H^o$= −40 kJ/mol) for condensation, which results in an increase of condenser duty [41]. The TUC of the direct sequence process was 7,829.06 kW, which showed an increase of 7.06% compared to the value of 7,312.60 kW of the two RD columns process. For approximately the same reactant extent and product purity, the case of two reactions occurring separately in the two respective RD columns is more efficient in terms of energy consumption than the case of two reactions occurring simultaneously in one RD column of the direct sequence. Even if the two reactions are intensified in one RD column of the direct sequence, the intensification does not bring energy savings. Thus, we propose a new configuration with internal heat integration by using the significant temperature difference between the two RD columns in Fig. 4.

2. Internally Heat-integrated Distillation Column

To further reduce the energy consumption in the two RD column process reported in the previous section, we developed an internally heat-integrated model by using the stage temperature gradient between the two RD columns due to the difference in reaction temperature. As shown in Fig. 4, the overall profile of the RD column temperature for 2-EHDEC production is higher than that of the RD column for MEDEC production. According to these temperature profiles, the RD column for the production of 2-EHDEC with high reaction temperature is called the HT column, and the RD column with low reaction temperature MEDEC production is called the LT column in the HIDiC configuration. The temperature gradient between two RD columns can cause heat transfer from the HT to LT column as the driving force of internal heat integration. Since the heat from the HT column with exothermic reaction is transferred to the LP column with endothermic reaction, both reactions can proceed in the forward direction. The two single RD columns were integrated into one column as a partially double annular structure as shown in Fig. 5. This structure can transfer the heat on the contact column shell between the inner and outer columns. The amount of heat transferred can be determined by the following equation:

$$Q = U \cdot A \cdot \Delta T_{eff} \tag{5}$$

The heat transfer coefficient (U) was set to 700 W/m^2·K, which was calculated as the average of the heat transfer coefficient of the concentric structure of HIDiC range of 600-800 W/m^2·K [42]. The surface area (A) of the contact region was equal to the surface area of the inner LT column surrounded by the outer HT column. With the diameter of the LT column (D=0.63 m) and the tray spacing of one stage (L=0.6096 m), the heat transfer area was calculated as 1.20 m^2. The temperature differences of overlapping stages (ΔT) could be obtained from the temperature profiles of a single RD column and are listed in Table 6.

In Fig. 4, the temperature profile shows that the stages near the reboiler have high operating temperature. To prevent the reversal of the temperature gradient direction between the LT and HT columns and maximize the heat transfer rate, all stages of two RD columns were matched in parallel. The minimum acceptable temperature difference between hot and cold regions is called the minimum temperature approach (ΔT_{min}) or pinch temperature [43,44]. ΔT_{min} is empirical data for an adequate heat transfer rate [32,45,

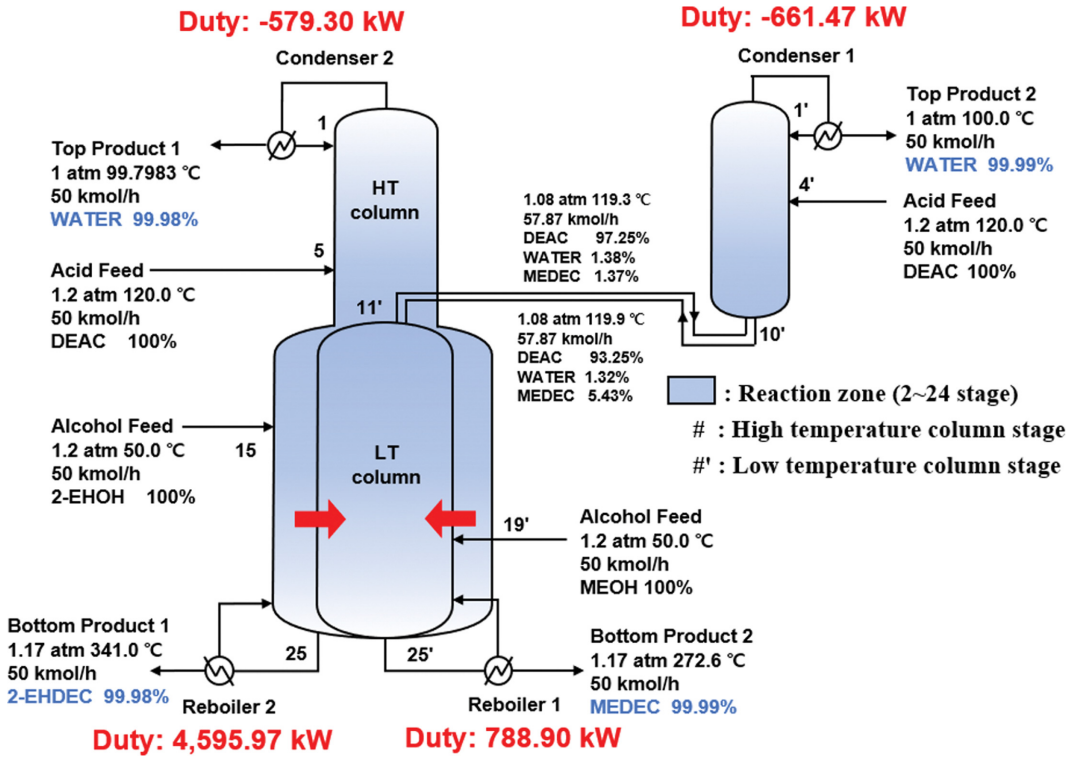

Fig. 5. Flowsheet of HIDiC as a partial double annular structure.

Table 6. Temperature profile and heat transfer rate of HIDiC

# of the overlapping stages	11	12	13	14	15	16	17	18	19	20	21	22	23	24
LT column temperature (°C)	108.31	103.46	99.26	97.97	97.74	97.72	97.57	95.55	72.04	72.2	72.36	72.56	79.18	209.83
HT column temperature (°C)	130.14	173.74	198.51	201.78	194.95	195.24	195.47	195.71	195.94	196.19	197.06	211.11	298.03	338.09
ΔT_{eff}	1.83	50.28	79.25	83.81	77.21	77.51	77.9	80.15	103.89	103.99	104.69	118.54	198.85	108.26
Heat transfer rate (kW)	1.54	42.47	66.93	70.78	65.21	65.46	65.79	67.69	87.74	87.83	88.42	100.12	167.94	91.43

46]. In this study, ΔT_{min} was set to 20 °C, and valid heat transfer occurs only in the overlapping stages to have $\Delta T > 20$ °C. Therefore,

$$\Delta T_{eff} = \Delta T - 20\ ^{\circ}C \quad (6)$$

As a result, heat does not transfer effectively from the 2nd to 10th stages, which have $|\Delta T| < 20$ °C, as shown in Fig. 4. The temperature profiles from the 11th to 24th stages of the LT column and HT column with higher temperature difference than the pinch temperature of 20 °C are listed in Table 6. The heat transfer rates (Q) and the effective temperature difference (ΔT_{eff}) at each overlapping stage were calculated by using Eqs. (5) and (6), respectively. The largest amount of heat is transferred in the 23rd stage, where the largest temperature difference among the overlapping stages occurs. As shown in Fig. 5, the HIDiC configuration has a partially double annular structure overlapping from the 11th to 24th stages. The diameters of these stages of the HT column and LT column after heat integration were 1.828 m and 0.640 m, respectively. The new diameter of the annular HT column was set as 1.934 m by considering that the HT column surrounds part of the LT column. Details of the diameter calculation are provided in Supplementary Information. In the HT column, the 2nd to 10th stages, where the heat does not transfer effectively, do not need to be included in the double annular structure because it increases the diameter of outer column and this leads to higher capital cost. Therefore, they are separated from the double annular structure, as shown in Fig. 5, and this structure is referred to as a partial double annular structure. The diameter of these non-overlapping stages of the HT column was determined to be 0.519 m, which would be increased to 1.934 m in a double annular structure for heat transfer. That of the LT column, which is separated from the partial double annular column, was determined to be 0.521 m by satisfying its column internals of operating capacity.

We designed the HIDiC model to satisfy the same product purity as obtained for the two RD column process. The simulated model, which is area-equivalent to HIDiC, satisfied a stable operating range in all stages. The jet flooding factor of all stages was not over 80% and the approach to system limit was 39.55% to 63.45%, which is not extreme and is in the feasible range. Both the reflux ratio and boilup ratio of LT and HT column were reduced in the HIDiC compared to the two RD column process. In Table 3, the reflux ratio of the LT and HT columns was reduced from 0.30 to 0.17 and from 0.49 to 0.00039, respectively, by the internal heat integra-

tion. The product purity in the HIDiC was 99.99 mol% and the reaction extent of both reactions was sufficiently high (above 49.99 kmol/h), as shown in Table 4. This means that the HIDiC achieved the same product purity even with a low reflux and boilup ratio. Since heat was transferred from the lower stages of the HT column as well, it is necessary to supply additional heat to the HT column reboiler for boiling the bottom stream. Therefore, the reboiler heat duty of the HT column of the HIDiC (4,595.97 kW) is higher than that of the single RD (3,803.69 kW) in Table 5. However, the reboiler duty of the LT column was significantly reduced and thus the total energy consumption of the HIDiC (6,625.64 kW) was reduced by 9.39% and 15.4% compared to the two RD column process and the conventional direct sequence, respectively.

The external heat integration was also designed for comparison with the HIDiC process. For the two RD column process with external heat integration, heat was transferred from the 2-EHDEC stream (341.0 °C) to the MEDEC stream (272.6 °C) in the heat exchanger. The transferred heat can offload the reboiler duty of the LT column by reducing the boilup ratio in the reboiler. However, it caused an adverse effect of increasing the reboiler duty of the HT column section. The TUC of the sequence with external heat integration was 8,330.97 kW, which is 13.9% higher than that of the two RD column process and 25.7% higher than that of HIDiC. The details of external heat integration are described in Supplementary Information.

3. Comparison between HIDiC and RDWC

To confirm the competitiveness of HIDiC, we designed one more heat-integrated configuration, RDWC, which integrates reactions in DWC. The optimization procedure described in a previous study was used [17]. The RDWC consisted of a reactive section for reac-

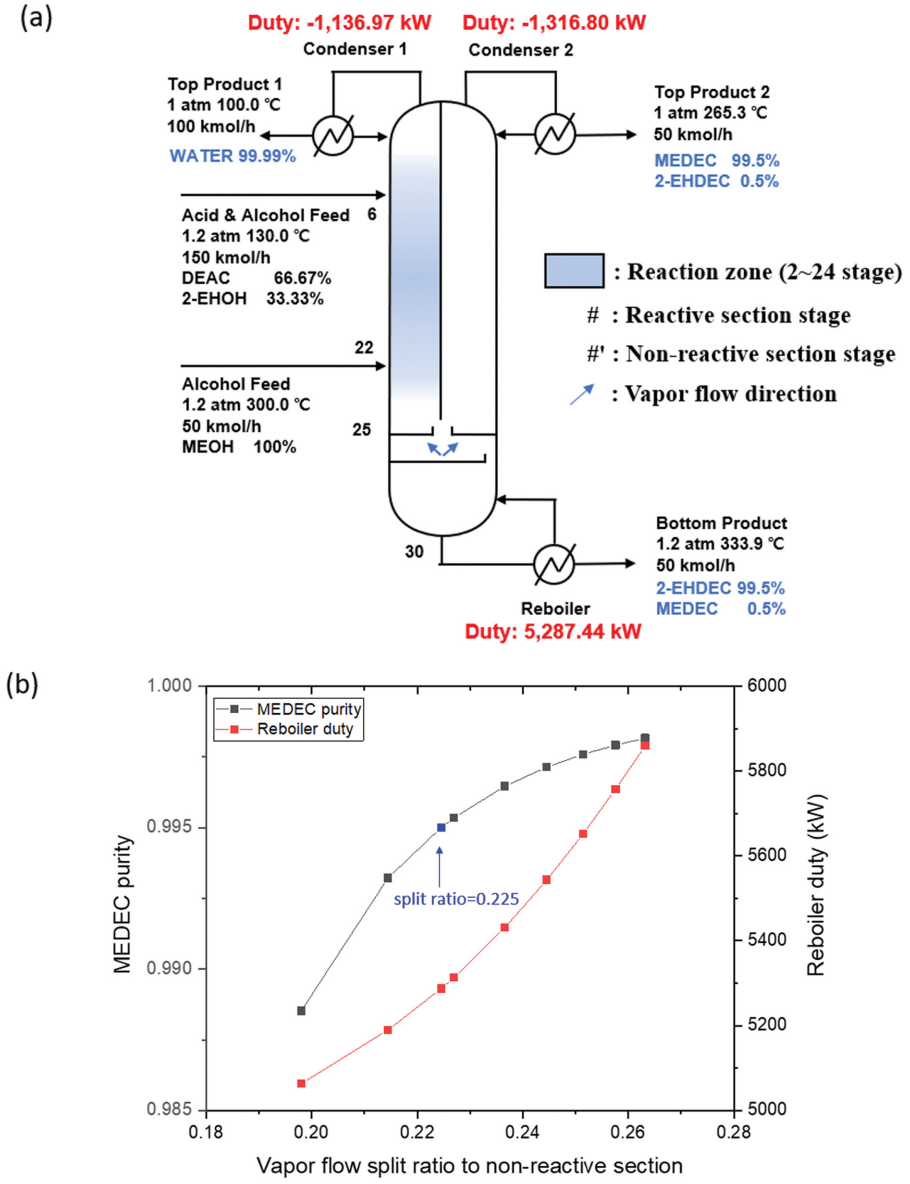

Fig. 6. (a) Flowsheet of RDWC (b) Sensitivity analysis of methyl dodecanoate purity and reboiler duty by varying the vapor flow split ratio to the non-reactive section.

Table 7. Total annual cost (TAC) of all processes

	Single RD	Direct sequence	HIDiC	RDWC
Total capital cost ($10^3$$)	2,060.51	1,913.19	1,905.98	2,283.69
Column vessel	592.08	539.27	541.33	920.34
Heat exchanger*	1,468.43	1,373.92	1,364.65	1,363.35
Total operating cost ($10^3$$/yr)	2,976.18	2,896.20	2,763.72	2,871.34
TAC ($10^3$$/yr)	3,663.02	3,533.93	3,399.04	3,632.57

*Capital cost of condenser and reboiler.

tion and a non-reactive section for product separation, divided by a wall. In the case of the RDWC, both the upper RDWC and lower RDWC were simulated. In the upper RDWC (Fig. 6(a)), the reflux ratio of a condenser in the reactive section was 0.0055 and that in the non-reactive section was 0.802. The vapor flow rate divided into reactive and non-reactive sections was determined by a sensitivity analysis. As shown in Fig. 6(b), as the vapor flow split ratio to the non-reactive section increases, the purity of MEDEC increases, but the reboiler duty of the RDWC process also increases. Therefore, we set the vapor flow split ratio to 0.225, which represents the lowest energy consumption in the ratio range that satisfies all product purity above 99.5 mol%. The vapor flow rate entering the reactive section is 255.29 kmol/h and that entering the non-reactive section is 73.93 kmol/h.

In the case of the lower RDWC, despite the higher energy consumption than the other processes, reactants were not consumed completely and the separation efficient was still low. Increasing the internal flow rate between the reactive section and non-reactive section can improve the product purity but requires high energy consumption. The maximum purity of MEDEC is 93.4 mol% with an optimal liquid flow split ratio of 0.181 (refer to the Supplementary Information). Thus, we considered only the upper RDWC in this study since the lower RDWC had no advantage compared to the other processes.

Like the other processes, reaction extent in the upper RDWC was also over 49.99 kmol/h. However, the product purity of the two esters in the RDWC (99.5 mol%) was significantly lower than the two RD column process. The maximum product purity is 99.82 mol% when the vapor flow split ratio to the non-reactive section is 0.263 and it consumes 5,859.88 kW of energy in reboiler, which is 10.29% higher than that to achieve the purity of 99.5 mol%. In Table 5, even the RDWC consumes less energy than the direct sequence but still requires more energy consumption than the HIDiC. The reboiler duty of the RDWC was 5,287.44 kW, which is similar to the sum of the reboiler duties of the HIDiC. However, like the direct sequence, the sum of condenser duties of the RDWC increased to 1.98 times that of the HIDiC due to the high molar flowrate handled in the condensers and the separation of the more difficult components to liquefy. The TUC of the RDWC was 7,741.21 kW, up 5.86% and 16.84%, respectively, compared to the two RD column process and HIDiC.

ECONOMIC EVALUATION

The TAC of each process with a payback period of three years is compared in Table 7. The details of the TAC evaluation are described in Supplementary Information. In the direct sequence, both the capital and the operating cost were reduced compared to the two RD column process. A process with high TUC also has high operating cost in common but the direct sequence in this study was not. In this study, since the high-pressure (HP) steam has insufficient temperature (254 °C) to boil ester products with high boiling temperature (334.497 °C, 266.624 °C), we used electricity of $16.8/GJ in the reboiler instead of HP steam [47]. In the direct sequence, the sum of reboiler duties (5,325.78 kW) is lower than that of the two RD column process (5,735.24 kW). The reduction of electricity usage in the direct sequence led to a significant reduction in the total operating cost. The capital cost of the column vessel was also reduced since the diameter of the non-RD column of the direct sequence decreased significantly. The diameters of each process are listed in Table 3. The TAC of the direct sequence was reduced by 3.52% compared to the two RD column process.

The HIDiC was designed to have the same active and downcomer area as a single RD column. A new diameter that satisfies the hydraulic conditions of the column was calculated through the dimensional analysis in Supplementary Information. Changed diameters of the inner and outer columns due to the internal heat integration were considered in the calculation of capital cost. Both the capital and the operating costs were reduced in the HIDiC compared to the two RD column process. Therefore, the TAC of the HIDiC was $\$3{,}399.04\times10^3$/yr, a reduction of 7.21% compared to the two RD column process. For the RDWC, due to the increase of the diameter of the column with the dividing wall and number of stages in the non-reactive section, the capital cost of the column vessel increased significantly from $\$592.08\times10^3$ to $\$920.34\times10^3$. However, considering the three year payback period, the TAC was reduced by 0.83% compared to the two RD column process due to the reduced total operating cost. Overall, the HIDiC showed the lowest TAC among all processes.

CONCLUSION

This study introduces an alternative design for effective energy savings by internal heat integration in a partial double annular column. The two RD column process has two respective columns where each single esterification reaction occurs in a separate RD column, while the direct sequence has one RD column where the two reactions take place, followed by a non-RD column. Since the direct sequence cannot reduce the energy consumption of the two RD column process having significantly different reaction tem-

peratures, we have derived a single partial double annular RD column (HIDiC) with internal heat integration of a high-temperature exothermic RD section and a low-temperature endothermic RD section. While the pinch pressure utilizes the temperature difference in the pressure-swing azeotropic distillation system, this study harnesses the operating temperature gradient between two RD columns as the driving force of heat transfer. Effective energy reduction is possible by using the significant temperature difference of two reaction systems. While satisfying the same reaction extent and product purity, the TUC of HIDiC was reduced by 15.4% and 14.4% compared to the direct RD sequence and RDWC.

ACKNOWLEDGEMENTS

This work was performed under the framework of the Research and Development Program of the Korea Institute of Energy Research (KIER) (C0-2427-03).

ABBREVIATIONS AND ACRONYMS

DEAC : dodecanoic acid [-]
DWC : dividing wall column [-]
HIDiC : internally heat-integrated distillation column [-]
HP : high-pressure [-]
HT : high-temperature [-]
LT : low-temperature [-]
MEDEC : methyl dodecanoate [-]
MEOH : methanol [-]
RD : reactive distillation [-]
RDWC : reactive dividing wall column [-]
SZ : sulphated zirconia [-]
TAC : total annual cost [$10^3$$/yr]
TUC : total utility consumption [kW]
VRHP : vapor recompression heat pump [-]
2-EHDEC : 2-ethylhexyl dodecanoate [-]
2-EHOH : 2-ethylhexanol [-]

Nomenclature

A : heat transfer area [m^2]
C_{cat} : molar concentration of catalyst [m^{-3}]
D : diameter of a column [m]
ΔH : heat of reaction [kJ/mol]
$\Delta_{liq}H^o$: standard liquefaction enthalpy [kJ/mol]
K_a : activity-based equilibrium constant [-]
k_C^* : rate constant of catalytic term [kmol m^{-6} s^{-1}]
k_U^* : rate constant of uncatalytic term [kmol m^{-6} s^{-1}]
k_1 : rate constant of forward reaction [kmol kg^{-1} s^{-1}]
k_{-1} : rate constant of reverse reaction [kmol kg^{-1} s^{-1}]
L : try spacing of one stage [m]
N_{RX} : reaction stages [-]
N_{Total} : number of total stages [-]
NF_{ACID} : feed stage of acid [-]
NF_{OH} : feed stage of alcohol [-]
Q : heat transfer rate [W]
ΔT : temperature differences of overlapping stages [°C]
ΔT_{eff} : effective temperature difference [°C]
ΔT_{min} : minimum temperature approach [°C]
U : heat transfer coefficient [W/m^2·K]
V_M : molar liquid volume [m^3]

Greek Letters

a_i : liquid activity [-]

SUPPORTING INFORMATION

Additional information as noted in the text. This information is available via the Internet at http://www.springer.com/chemistry/journal/11814.

REFERENCES

1. F. I. Gomez-Castro, V. Rico-Ramirez, J. G. Segovia-Hernandez and S. Hernandez, *Chem. Eng. Process. Process Intensif.*, **49**, 262 (2010).
2. G. M. Kim, W. Y. Choi, J. H. Park, S. J. Jeong, J.-E. Hong, W. Jung and J. W. Lee, *ACS Appl. Nano Mater.*, **3**, 8592 (2020).
3. N. V. D. Long, D. Y. Lee, T. H. Han, P. Sunyong, H. B. Bong and M. Lee, *Korean J. Chem. Eng.*, **37**, 1823 (2020).
4. R. J. Galanido, D. S. Kim and J. Cho, *Korean J. Chem. Eng.*, **37**, 850 (2020).
5. Z. Jiang and R. Agrawal, *Chem. Eng. Res. Des.*, **147**, 122 (2019).
6. M. F. Malone and M. F. Doherty, *Ind. Eng. Chem. Res.*, **39**, 3953 (2000).
7. A. A. Kiss, M. Jobson and X. Gao, *Ind. Eng. Chem. Res.*, **58**, 5909 (2019).
8. J. W. Lee, S. Hauan and A. W. Westerberg, *Ind. Eng. Chem. Res.*, **39**, 1061 (2000).
9. J. W. Lee and A. W. Westerberg, *AIChE J.*, **47**, 1333 (2001).
10. R. S. Huss, F. Chen, M. F. Malone and M. F. Doherty, *Comput. Chem. Eng.*, **27**, 1855 (2003).
11. S. B. Gadewar, M. F. Malone and M. F. Doherty, *Ind. Eng. Chem. Res.*, **46**, 3255 (2007).
12. J. W. Lee, S. Hauan and A. W. Westerberg, *AIChE J.*, **46**, 1218 (2000).
13. J. W. Lee, S. Hauan, K. M. Lien and A. W. Westerberg, *Proc. R. Soc. A*, **456**, 1953 (2000).
14. J. W. Lee, S. Hauan, K. M. Lien and A. W. Westerberg, *Proc. R. Soc. A*, **456**, 1965 (2000).
15. I. Dejanović, L. Matijašević and Ž. Olujić, *Chem. Eng. Process.*, **49**, 559 (2010).
16. Ö. Yildirim, A. A. Kiss and E. Y. Kenig, *Sep. Purit. Technol.*, **80**, 403 (2011).
17. W. Jang, H. Lee, J.-i. Han and J. W. Lee, *Ind. Eng. Chem. Res.*, **58**, 8206 (2019).
18. W. Jang, K. Namgung, H. Lee, H. Mo and J. W. Lee, *Ind. Eng. Chem. Res.*, **59**, 1966 (2020).
19. I. Mueller and E. Y. Kenig, *Ind. Eng. Chem. Res.*, **46**, 3709 (2007).
20. F. J. Novita, H.-Y. Lee and M. Lee, *Korean J. Chem. Eng.*, **35**, 926 (2018).
21. S. Feng, Q. Ye, H. Xia, R. Li and X. Suo, *Chem. Eng. Res. Des.*, **125**, 204 (2017).
22. A. Yang, S. Sun, A. Eslamimanesh, S. a. Wei and W. Shen, *Energy*, **172**, 320 (2019).
23. K. Namgung, H. Lee, W. Jang, H. Mo and J. W. Lee, *Chem. Eng.*

Process. Process Intensif., **154**, 108048 (2020).
24. H. Mo, H. Lee, W. Jang, K. Namgung and J. W. Lee, *Korean J. Chem. Eng.*, **38**, 195 (2021).
25. A. Harwardt and W. Marquardt, *AIChE J.*, **58**, 3740 (2012).
26. H. Lee, W. Jang and J. W. Lee, *Korean J. Chem. Eng.*, **36**, 954 (2019).
27. J. Fang, X. Cheng, Z. Li, H. Li and C. Li, *Chin. J. Chem. Eng.*, **27**, 1272 (2019).
28. M. Gadalla, L. Jiménez, Z. Olujic and P. J. Jansens, *Comput. Chem. Eng.*, **31**, 1346 (2007).
29. T. Glenchur and R. Govind, *Sep. Sci. Technol.*, **22**, 2323 (1987).
30. K. Naito, M. Nakaiwa, K. Huang, A. Endo, K. Aso, T. Nakanishi, T. Nakamura, H. Noda and T. Takamatsu, *Comput. Chem. Eng.*, **24**, 495 (2000).
31. M. Nakaiwa, K. Huang, A. Endo, T. Ohmori, T. Akiya and T. Takamatsu, *Chem. Eng. Res. Des.*, **81**, 162 (2003).
32. H. Lee, H. Mo, K. Namgung, W. Jang and J. W. Lee, *Ind. Eng. Chem. Res.*, **59**, 14398 (2020).
33. F. Omota, A. C. Dimian and A. Bliek, *Chem. Eng. Sci.*, **58**, 3159 (2003).
34. F. Omota, A. C. Dimian and A. Bliek, *Chem. Eng. Sci.*, **58**, 3175 (2003).
35. S. Steinigeweg and J. Gmehling, *Ind. Eng. Chem. Res.*, **42**, 3612 (2003).
36. M. Hino, M. Kurashige, H. Matsuhashi and K. Arata, *Thermochim. Acta*, **441**, 35 (2006).
37. M. A. Alves-Rosa, L. Martins, P. Hammer, S. H. Pulcinelli and C. V. Santilli, *RSC Adv.*, **6**, 6686 (2016).
38. R. Lamba, S. Kumar and S. Sarkar, *Chem. Eng. Commun.*, **205**, 281 (2018).
39. M. F. Doherty, *Chem. Eng. Sci.*, **40**, 1885 (1985).
40. Y.-C. Wu, H.-Y. Lee, C.-Y. Tsai, H.-P. Huang and I. L. Chien, *Comput. Chem. Eng.*, **57**, 63 (2013).
41. A. C. G. van Genderen, J. C. van Miltenburg, J. G. Blok, M. J. van Bommel, P. J. van Ekeren, G. J. K. van den Berg and H. A. J. Oonk, *Fluid Phase Equilib.*, **202**, 109 (2002).
42. A. A. Kiss and Ž. Olujić, *Chem. Eng. Process.*, **86**, 125 (2014).
43. B. Linnhoff and E. Hindmarsh, *Chem. Eng. Sci.*, **38**, 745 (1983).
44. M. Gadalla, Z. Olujic, L. Sun, A. De Rijke and P. J. Jansens, *Chem. Eng. Res. Des.*, **83**, 987 (2005).
45. B.-H. Li, Y. E. Chota Castillo and C.-T. Chang, *Chem. Eng. Res. Des.*, **148**, 260 (2019).
46. B.-H. Li and C.-T. Chang, *Ind. Eng. Chem. Res.*, **49**, 3967 (2010).
47. W. L. Luyben, *Distillation design and control using aspen simulation*, John Wiley & Sons, Hoboken, New Jersey (2013).

Supporting Information

Temperature driven internal heat integration in an energy-efficient partial double annular column

Chaeyeong Seo, Heecheon Lee, Minyong Lee, and Jae W. Lee†

Department of Chemical & Biomolecular Engineering, Korea Advanced Institute of Science and Technology (KAIST), 291 Daehak-ro, Daejeon 34141, Korea

(*Received 15 March 2021 • Revised 4 August 2021 • Accepted 24 August 2021*)

1. Assumptions for Reaction Kinetics and Modeling

- The combustion enthalpy of a 2-ethylhexyl dodecanoate was calculated using the bond energy.
- The Amberlyst 15 is assumed thermally stable in a reactive distillation column of the direct sequence as the operating temperature of all stages are under 120 °C except for two bottom stages.
- The heat transfer coefficient of 700 W/m^2K which is the average of the heat transfer coefficient range of the concentric structure (600-800 W/m^2K)[1] was used.

2. Calculation of Enthalpy of Reactions

The enthalpies of the esterification reaction were calculated using the combustion enthalpies of each components. The combustion enthalpies in Table S1 were obtained from Aspen Plus™ and the insufficient data for 2-EHDEC was calculated using the bond energy by assuming ideal interaction.

3. Determination of Total Stage Number in Design Basis

This study considered the heat transfer in the determination of N since the design basis of a single distillation column was also used for the internal heat-integrated column. Fig. S1(a) to (c) shows the temperature profile of two reactive distillation columns (HT and LT column). Regardless of the total stage number (N), two columns have a region in top stages with little change in temperature. Due to the insignificant temperature difference between two columns, the heat transfer cannot effectively occur in this region. Thus, only the remaining stages below this region are considered as overlapping stages for possible heat transfer.

If N of each column is not the same in general, the smaller stage number is the limiting constraint that determines the number of overlapping stages. In Fig. S1(a) and (b), the overlapping stages was determined as the remaining stages of the column with small N even with the different overlapping region. Therefore, the N of the two columns was set to be equal in this study.

In order to determine N, we performed a sensitivity analysis of the total utility consumption of the internal heat-integrated model according to N. As shown in Fig. S1(d), the model has the lowest energy consumption at N=25. In the case of N over 25, the heat duty of the HT column reboiler was dramatically increased to recover the lost heat by using additional energy consumption. Therefore, we selected N=25 as the most suitable number of stages for efficient internal heat-integration.

4. Single RDs with External Heat Integration

For the external heat integration, the bottom stream of HT column (2-EHDEC) enters as a hot stream and the bottom stream of LT column (MEDEC) enters as a cold stream. The transferred heat boils up the product in the reboiler and reduce the reboiler duty. As shown in Fig. S2, the reboiler duties of two single RD columns with external heat integration are 370.64 kW and 5,625.69 kW. Although the reboiler duty of LT column is significantly reduced, that of HT column increases by 148% compared to before external heat integration. By depriving the heat, the reboiler in HT column needs additional heat to boil the bottom stream. Therefore, the TUC of the single RD process with external heat integration is 8,330.98 kW which is 13.9% and 25.7% higher than the cases of the single RD process (7,312.60 kW) and HIDiC 6,625.64 kW), respectively.

5. Simulation Result of Lower RDWC

For lower RDWC in Fig. S3, the number of total stages is 30 and the reaction are from 7th to 29th stages. DEAC and 2-EHOH are fed to 20th stage and MEOH is fed to 24th stage. The reflux ratio of the condenser and the boilup ratios of the two reboilers were determined to 7, 12.42 and 0.07, respectively. The liquid flow rate entering the reactive section is 258.73 kmol/h, and the non-reactive section is 52 kmol/h. These settings were for the maximum product purities, 96.7 mol% of WATER, 93.4 mol% of MEDEC and

Table S1. Energy of combustion

Reaction	H (kJ/mol)
[a] $C_{11}H_{23}COOH+17O_2 \leftrightarrow 12CO_2+12H_2O$	−6,850
[a] $C_8H_{17}OH+12O_2 \leftrightarrow 8CO_2+9H_2O$	−4,892
[a] $C_{11}H_{23}\text{-}COO\text{-}C_8H_{17}+37/2O_2 \leftrightarrow 13CO_2+13H_2O$	−7,566.8
[a] $CH_3OH+3/2O_2 \leftrightarrow CO_2+2H_2O$	−638.2
[b] $C_{11}H_{23}\text{-}COO\text{-}CH_3+29O_2 \leftrightarrow 20CO_2+20H_2O$	−11,731

[a]Aspen Plus data

[b]Calculated data by bond energy[2]

[1]A. A. Kiss, Ž. Olujić, A review on process intensification in internally heat-integrated distillation columns. *Chemical engineering and processing: process intensification* (2014).

[2]Kildahl, N. K., Bond energy data summarized, *Journal of chemical education* (1995).

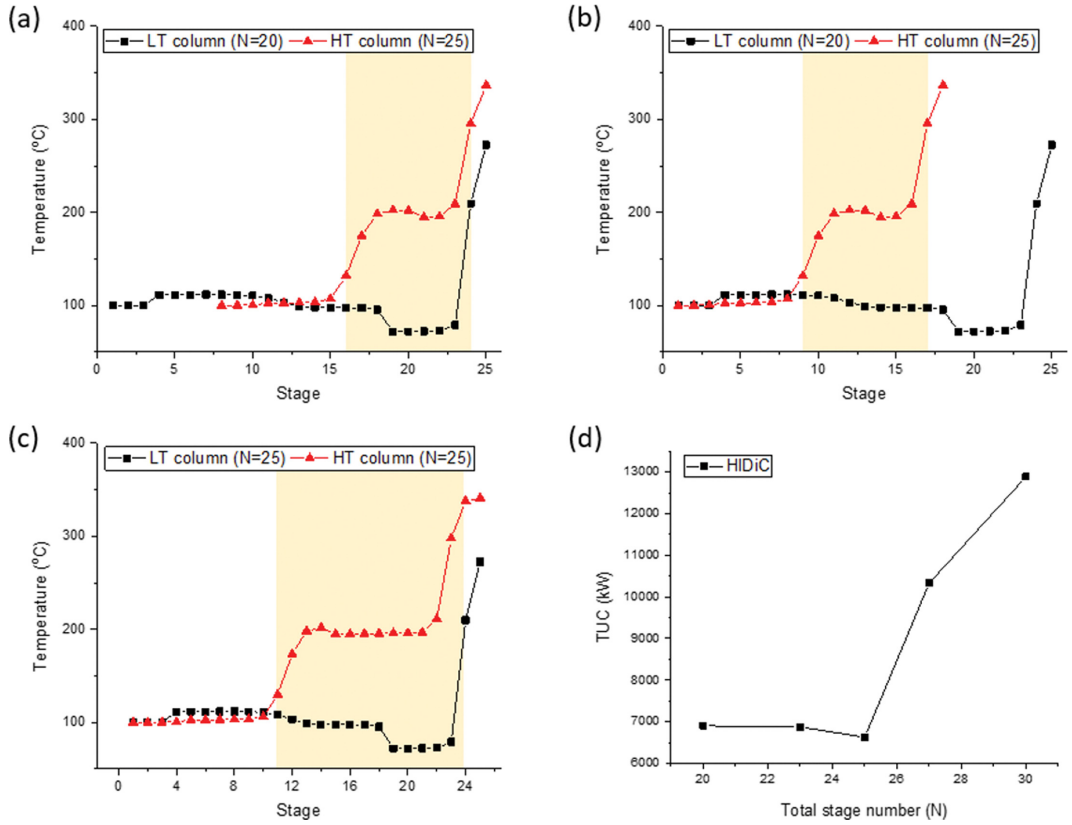

Fig. S1. The temperature profiles of two reactive distillation columns (HT and LT columns) (a) with different N overlapping in the bottom stages, (b) in the top stages, and (c) with the same N, (d) the total utility consumption of the internal heat integrated model according to N.

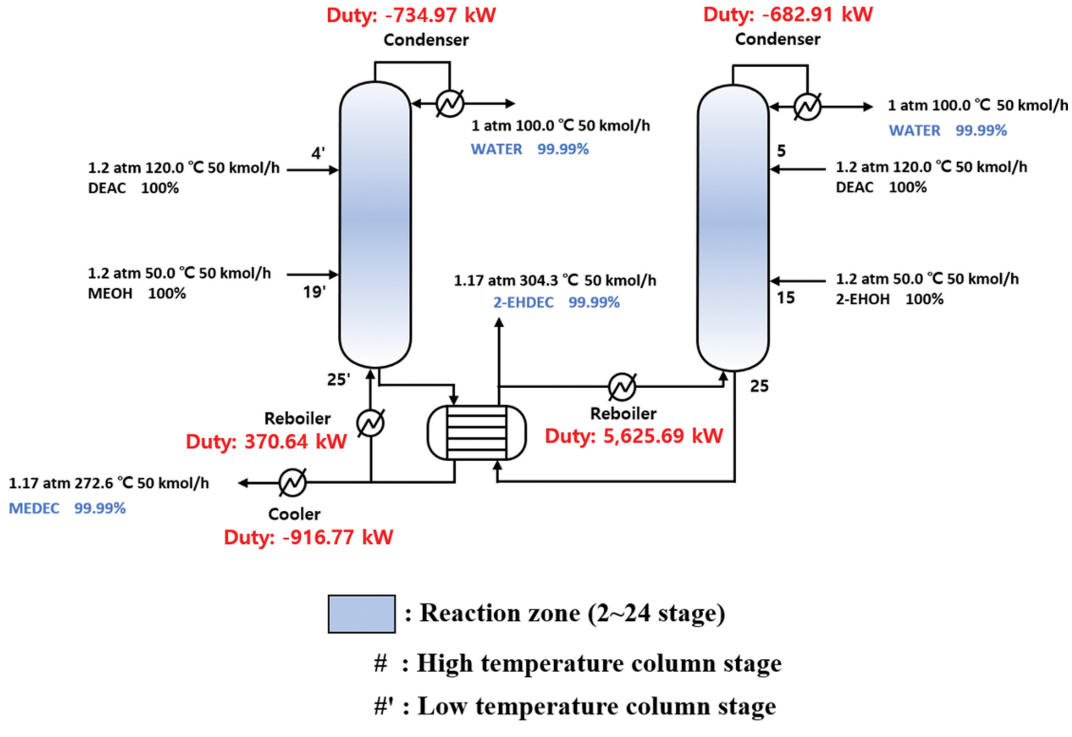

Fig. S2. Flowsheet of two RD columns process with external heat integration.

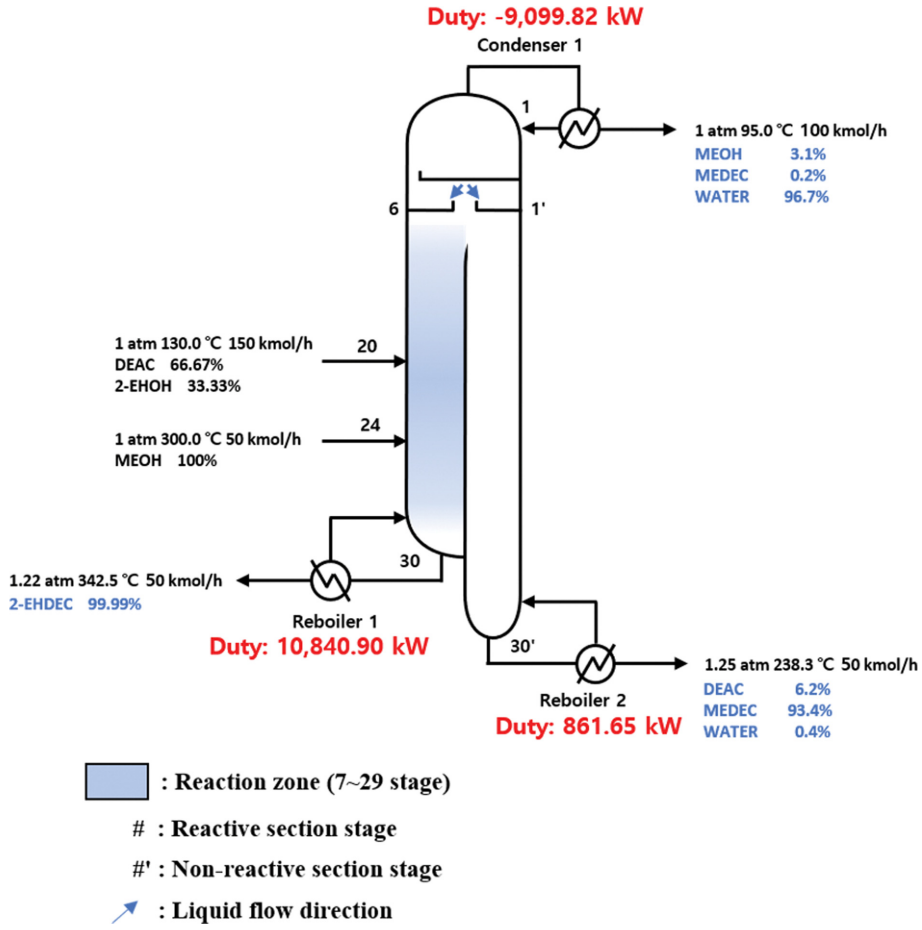

Fig. S3. Flowsheet of lower RDWC.

99.99 mol% of 2-EHDEC. The lower RDWC required 20,802.37 kW which is 268.72% of that of the upper RDWC.

6. Dimension Analysis

Since HIDiC has a double annular structure in which the HT column surrounds the LT column, new diameter is calculated. The active are of the traditional tray in single RD can be calculated as follows:

$$A = \pi\left(\frac{D}{2}\right)^2 \tag{S1}$$

In order to satisfy the equivalent active area of outer tray of HIDiC, the diameter of annular tray (D_a) has a relation with the diameter of the LT column (D_l) and the HT column (D_h) in single RDs.

$$\pi\left(\frac{D_h}{2}\right)^2 = \pi\left(\frac{D_a}{2}\right)^2 - \pi\left(\frac{D_l}{2}\right)^2 \tag{S2}$$

It can be rearranged with the expression for D_a.

$$D_a = 2\sqrt{\left(\frac{D_l}{2}\right)^2 + \left(\frac{D_h}{2}\right)^2} \tag{S3}$$

Since D_l=0.630 m and D_h=1.828 m, D_a was calculated as 1.934 m.

7. Cost Evaluation

The TAC was calculated with payback period of 3 years as follows:

$$TAC = \frac{\text{Total capital cost}}{3} + \text{Total operating cost}$$

The interest rate, depreciation rate, and tax rate are assumed to be negligible since the capital cost and the operating cost for energy consumption are more significant considerations. Total capital cost for each process is sum of the capital cost of column vessels, condensers and reboilers of each column in Eq. (S4)-(S6). The required values for TAC calculation such as heat duty (Q_c, Q_r) and the diameter (D) can be obtained in simulation result and column sizing in Aspen Plus™, respectively.

$$\text{Column vessel capital cost} = 17{,}640\,(D)^{1.066}\,(L)^{0.802} \tag{S4}$$

where D is a dimeter of the column and L is a height of the column

$$\text{Condenser capital cost (\$)} = 7{,}296\left(\frac{Q_c}{U_c \Delta T}\right)^{0.65} \tag{S5}$$

$$\text{Reboiler capital cost (\$)} = 7{,}296\left(\frac{Q_r}{U_r \Delta T}\right)^{0.65} \tag{S6}$$

where U_c=852 W/m^2·K, U_r=568 W/m^2·K

The operating cost of condenser and reboiler was calculated in Eq. (S7)-(S8). The reboiler commonly uses LP, MP and HP steam in Table S2 to boil up liquid streams at the bottom, but our prod-

Table S2. Costs of utilities

Utility	Cost ($/GJ)[3]
LP steam (6 bar, 433 K)	7.78
MP steam (11 bar, 457 K)	8.22
HP steam (42 bar, 527 K)	9.88
Electricity	16.8
Chilled water (278 K)	4.43

Table S3. Total annual cost (TAC) of all processes with 5 years of payback period

	Single RD	Direct sequence	HIDiC	RDWC
Total capital cost ($10^3$$)	2,060.51	1,913.19	1,905.98	2,283.69
Column vessel	592.08	539.27	541.33	920.34
Heat exchanger*	1,468.43	1,373.92	1,364.65	1,363.35
Total operating cost ($10^3$$/yr)	2,976.18	2,896.20	2,763.72	2,871.34
TAC ($10^3$$/yr)	3,388.28	3,278.84	3,144.92	3,328.08

*Capital cost of condenser and reboiler.

ucts have a very high boiling point so that cannot be boiled with those steams. Therefore, relatively high prices of electricity were used. We used 5 °C chilled water for condensing which costs $4.43/GJ and electricity for reboiling which costs $16.8/GJ.

$$\text{Condenser operating cost (\$/yr)} = \$4.43/\text{GJ} \cdot Q_c\ (\text{GJ/h}) \cdot 8{,}000\ \text{h/yr} \quad \text{(S7)}$$

$$\text{Reboiler operating cost (\$/yr)} = \$16.8/\text{GJ} \cdot Q_r\ (\text{GJ/h}) \cdot 8{,}000\ \text{h/yr} \quad \text{(S8)}$$

The TAC evaluation with 5 years of payback period in Table S3 shows that HIDiC had the lowest TAC as with that of 3 years.

[3]W. L. Luyben, *Distillation design and control using Aspen simulation*, John Wiley & Sons (2013).